Reliability of Soil Sublayers under Earth Quake Excitation

markov approach

Nielsen, Søren R. K.; Thoft-Christensen, P.; Jacobsen, H. Moust

Published in:
Proc. of the IV Int. Conf. Soil Dynamics and Earthquake Engineering

Publication date:
1989

Document Version
Early version, also known as pre-print

Reliability of Soil Sublayers under Earthquake Excitation: Markov Approach. Structural Dynamics and Soil Structure Interaction, pp. 19 - 37. Proceedings of the IV Int. Conf. Soil Dynamics and Earthquake Engineering. Mexico City. Oct. 1989.

[63]

RELIABILITY OF SOIL SUBLAYERS UNDER EARTHQUAKE EXCITATION: MARKOV APPROACH

S. R. K. Nielsen*, P. Thoft-Christensen* and H. Moust Jacobsen**

**Institute of Building Technology and Structural Engineering, University of Aalborg, Sohngaardsholmsvej 57, DK-9000 Aalborg, Denmark*

***Department of Civil Engineering, Laboratory of Soil Mechanics, University of Aalborg, Sohngaardsholmsvej 57, DK-9000 Aalborg, Denmark*

ABSTRACT

A single-degree-of-freedom hysteretic model is formulated for a subsoil layer subjected to earthquake excitation, using a Bouc-Wen model for the incremental constitutive equation of the hysteretic shear stress. The horizontal earthquake acceleration process at bedrock level is modelled as a non-stationary white noise, filtered through a time-invariant linear second order filter. Liquefaction is studied in triaxial tests, and is considered as a failure event. By cyclic loads it is shown that liquefaction takes place, when the accumulated mechanical energy dissipated per unit volume of the soil exceeds a critical value. This quantity is then introduced as damage indicator. The state variables of the integrated dynamic system of the soil sublayer, auxiliary filter and damage indicator then make up a Markov vector. An equivalent linearization technique is used for the constitutive equation of the shear stress, whereas a cubic polynomial expansion is used for the damage indicator equation. The resulting infinite hierarchy of statistical moment equations is closed by a cumulant neglect closure scheme. The expectations appearing in the equations for the coefficients of the equivalent polynomia are calculated by a 2-dimensional Gram-Charlier expansion. The analytical results obtained are compared to those obtained by Monte-Carlo simulation.

INTRODUCTION

Based on cyclic triaxial tests, formulas for the pore pressure built up have been developed, [16]. The constitutive equations for the hysteretic stress-strain curves have been studied, [7], and a modified Bouc-Wen model, [8], has been set up. The accumulated mechanical energy dissipated in the soil is used as a damage indicator. It is a non-linear response quantity with non-decreasing sample curves, and it is a measure at a macroscopic scale of the strength and stiffness deterioration of the soil during hysteretic

deformations. Failure is defined to take place at the first passage of the damage indicator at a predefined critical level, at which the soil is assumed to lose all its strength and stiffness.

In accordance with common practice in earthquake engineering the excitation process at bedrock level is modelled by a linear filtering of a Gaussian white noise through a shaping filter, [1, 2].

The constitutive equation for the hysteretic shear stress is non-linear and non-analytic. Therefore an equivalent system is introduced, for which this equation is given by a linear expression with coefficients determined via a least-square procedure. For the damage indicator differential equation an equivalent cubic expansion is formulated based on a Taylor-expansion. Joint statistical moments of the non-zero mean Markov vector process are then determined from the equivalent polynomial system. This approach is considered a generalization of the equivalent linearization technique, for which the non-zero mean formulation is due to Spanos [3] and Baber [4]. Equivalent polynomial expansion techniques were formulated by Nielsen et al. [5] for the zero mean problem, and by Mørk [6] for the non-zero mean problem.

The main objective of the present study is to develop and verify the indicated approximate analytical technique to the considered problem. All analytical results are compared to those obtained by numerical simulation. A generalization of the indicated method to multi-layer subsoils is straightforward, modelling the subsoil layer by a multi-degree-of-freedom system.

SOIL SUBLAYER

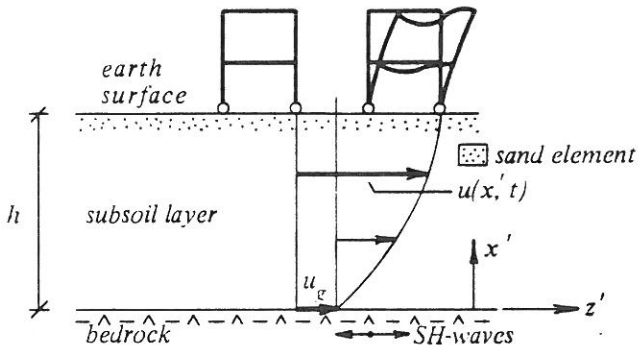

Figure 1. Displacement of subsoil layer subjected to earthquake.

A saturated sand layer of thickness h is assumed to cover a rock surface, as shown in fig. 1. During an earthquake shear waves (SH-waves) propagate from bedrock upwards through the sand layer. The horizontal displacements of the bedrock $u_g(t)$ and of the sandlayer $u(x', t)$ are as-

sumed to occur under plane strain conditions. x' is a vertical coordinate measured from the bedrock surface towards the free surface.

A sand element at the coordinate x' is consolidated under K_0-conditions prior to the earthquake. The effective mean normal stress p' is then

$$p' = \frac{1}{3}\,(1 + 2K_0)\,\sigma'_v \tag{1}$$

where σ'_v is the effective overburden pressure. During an earthquake shear stresses act on horizontal planes with irregularly varying sign and magnitude.

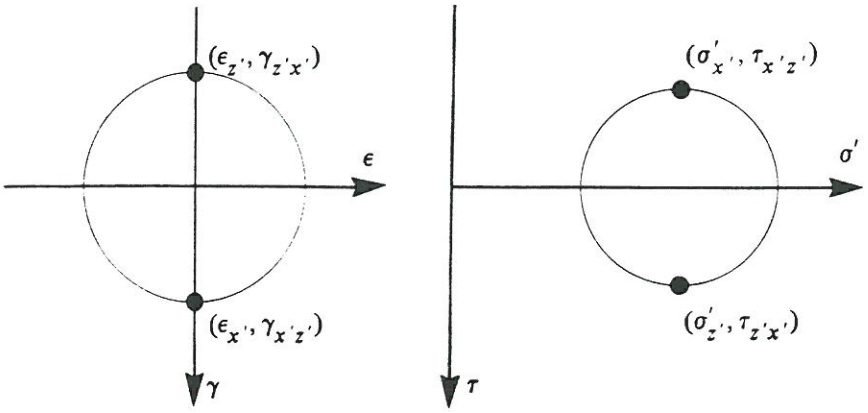

Figure 2. Mohr's circles for strains and stresses in a soil element during an earthquake.

The relation between in situ stresses and strains, and those existing in a triaxial test can be established as follows. In the horizontal or vertical planes no elongation takes place, and the volume changes $\epsilon_v = \epsilon_{x'} + \epsilon_{z'} = 0$ due to undrained circumstances and the absence of compression waves. The Mohr circles for the strains and stresses as shown in fig. 2 then give

$$\left.\begin{aligned} &\gamma_{x'z'} = \epsilon_1 \\ &\sigma'_{x'} = \sigma'_{z'} \\ &\tau_{x'z'} = \tfrac{1}{2}\,(\sigma'_1 - \sigma'_3) = \tfrac{1}{2}\,q \end{aligned}\right\} \tag{2}$$

where q is the deviatoric stress.

The dissipated effect per unit volume of soil is given by

$$\dot{E} \;=\; \sigma_{x'}\dot{\epsilon}_{x'} + \sigma_{z'}\dot{\epsilon}_{z'} + 2\tau_{x'z'}\dot{\gamma}_{x'z'} \;=\; q\,\dot{\epsilon}_1 \tag{3}$$

Field conditions still deviate from those developed during triaxial testings. The principal stresses rotate during an earthquake but are fixed

during cyclic loading, [13]. Further, in the field the soil behaves as a hysteretic material, but no permanent horizontal movements are developed in a systematic way. It is difficult to avoid irreversibilities in triaxial testing.

Cyclic Triaxial Tests

Test specimens:	Vestbjerg Sand	Lund No. 0
Mean diameter d (mm):	0.11	0.40
Uniformity U:	3.6	1.7
Void ratio e:	0.62	0.63
Density index I:	0.77	0.70

Table 1. Properties of test sands.

Cyclic triaxial tests with constant amplitude have been carried out on two sorts of sand, specified in table 1. The specimens have been fully saturated, using a total vacuum. which causes an isotropic preconsolidation pressure of 100 kPa. The test series and test results are described in further detail in ref. [7].

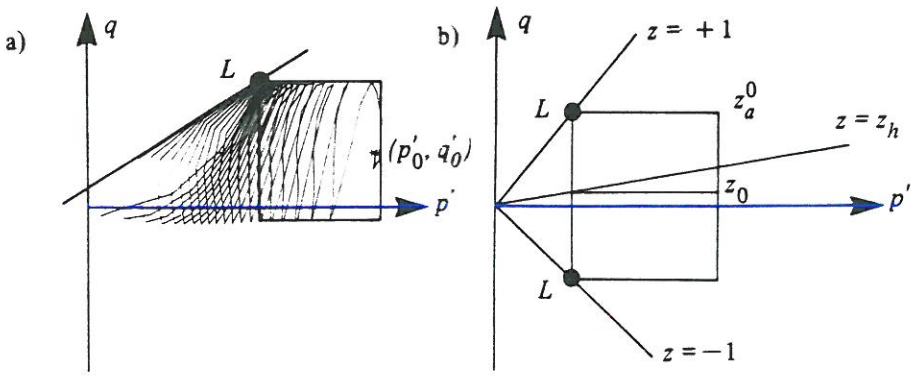

Figure 3. Cyclic triaxial tests. a) With initial, effective deviatoric stresses and irreversible strains. b) With reversible strain. Definition of mobilization factor z.

After consolidation at the initial stress state (p_0', q_0), the drains were closed and the specimens subjected to shear stresses with constant amplitudes, as shown in fig. 3a. During a single loading the mean normal stress p' varies only a little, corresponding to a small, but systematic increment in pore pressure. During a number of loadings the effective stress state then changes. If the Coulomb failure criterion is satisfied even once (point L in fig. 3a), the maximum shear stress decreases rapidly causing the sand to flow. The test equipment then loses control with the stress variation.

According to Casagrande [14] liquefaction is defined to take place if the stress state reaches the point L. The stress states may develop further

until strain amplitudes above 20% are reached. This state is designated complete liquefaction, Castro [15]. Only the development of stresses and strains until the point L is of practical interest, because even in this stress state the movements in a sand layer will damage all structures on its surface.

Mobilization Factor

The deviatoric stress q can be normalized by introducing a mobilization factor

$$z = \frac{q}{q_f}, \qquad z \in (-1, 1) \tag{4}$$

where q_f is the numerical maximum value of q at the actual mean normal stress p'.

The Coulomb failure criterion for a purely frictional material can be written

$$\left.\begin{array}{ll} q_f = \frac{6 \sin \varphi'}{3 - \sin \varphi} & \text{(compression)} \\ q_f = \frac{6 \sin \varphi'}{3 + \sin \varphi} & \text{(extension)} \end{array}\right\} \tag{5}$$

If the same deviatoric stress q is applied to compression and extension, corresponding to the initial mobilization factor $z_0 = 0$, large permanent deformations are developed in extension, a phenomenon called necking. In the field only hysteretic strains develop. The corresponding shear stresses in triaxial tests should occur simultaneously in compression and extension. From eq. (5) and fig. 3b it follows that $z_0 \in [0, z_h]$, where $z_h = sin\varphi'/(3 - sin\varphi')$.

Pore Pressure Build Up

The pore pressure build up causes a reduction in p' and q_f. Fig. 3b shows that the amplitude z_a then increases from its initial value z_a^0 to unity at point L. In [16] a formula has been developed for different values of the initial mobilization factor z_0. For $z_0 = 0$ this formula reads

$$z_a = z_a^0 \left(1 + R\, r(N)\right) \tag{6}$$

where R is a constant, and N is the number of cyclic loadings. $r(N) = 0$ for $N = 0$, increasing monotonically to $r(N) = 1$ for $N = \infty$.

Hysteretic Behaviour

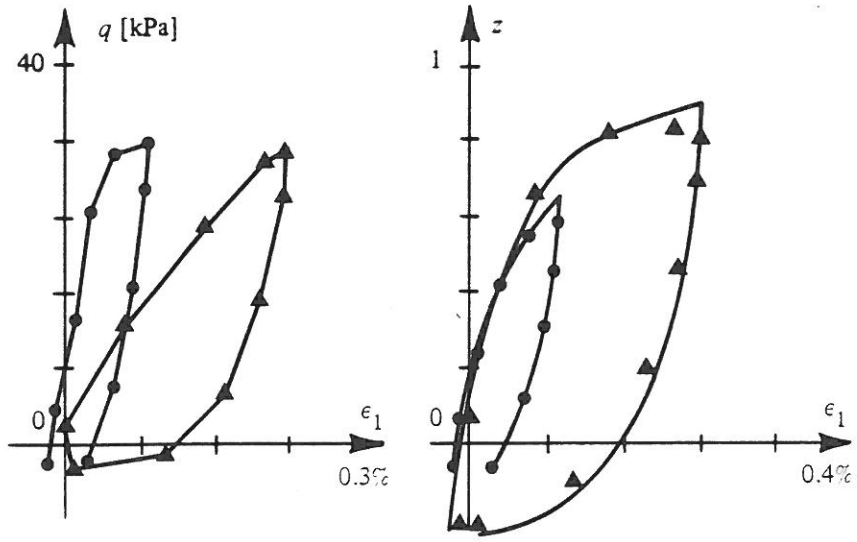

Figure 4. Hysteretic curves estimated from eq. (7), (8), (9), and measured in triaxial tests.

Figure 4a shows two test results. The behaviour of the sand is strongly hysteretic, but no irreversibility occurs. q_f and the elastic shear modulus μ_0 of the sand decrease from initial values $q_{f,0}$ and $\mu_{0,0}$ with the number of cycles as the pore pressure builds up. Simultaneously the development of the mobilization factor can be specified by the following modified Bouc-Wen formula, [8]

$$\dot{z} = k(\dot{x}, z)\, \dot{x} \tag{7}$$

$$k(\dot{x}, z) = 1 - \alpha\, sign(\dot{x})|z|^{n-1} z - \beta\, |z|^n \tag{8}$$

$$x = \frac{\mu_0}{q_f}\, \gamma_{x'z'} \tag{9}$$

Since z is restricted to the interval (-1,1), it is nescessary that $\alpha + \beta = 1$ in (8).

For all tests it has been found that μ_0 and q_f deteriorate proportionally, i.e. the fraction μ_0/q_f is constant with time. In equations (8),(9) it was found for all tests and even for different sorts of sand, that $\mu_{0,0}/q_{f,0} = 900$ with $\alpha = 1.0$, $\beta = 0.0$, $n = 0.5$.

Damage Indicator

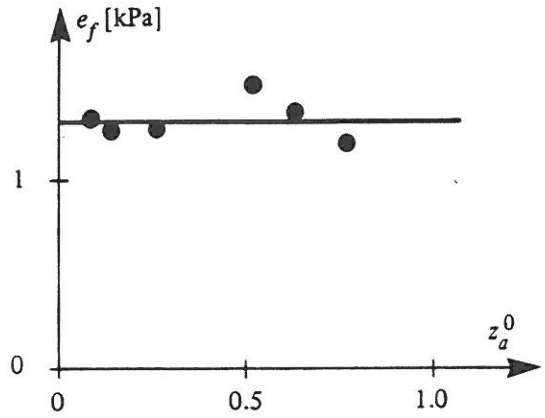

Figure 5. Energy dissipation per unit volume for $z = 0.98$, $\varphi' = 38°$, $p' = 25$ kPa. ($e_f = 0.2\,p'\ \sin\varphi'/(3 - \sin\varphi')$).

The dissipated accumulated energy under cyclic loading can be calculated from equations (3), (6), (7), (8), (9). At failure it turns out to be nearly constant, see fig. 5. This quantity is supposed to be constant even when the amplitude varies, and can then be used as a damage indicator. The accumulated dissipated energy will be normalized with respect to the quantity $\frac{1}{4}q_{f,0}^2/\mu_{0,0}$, which can be interpreted as the strain energy per unit volume, if elastic deformations were present up to the maximum shear stress $\frac{1}{2}q_{f,0}$. Using the time-invariance of $\mu_0(D)/q_f(D) = \mu_{0,0}/q_{f,0}$, and introducing the non-dimensional stress and strains defined by (4) and (9) in (3), the differential equation specifying the development of the damage indicator can be written

$$\dot{D} = 4\ f(D)\ z\dot{x} \tag{10}$$

where the following non-dimensional function is introduced

$$f(D) = \frac{\mu_0(D)}{\mu_{0,0}} = \frac{q_f(D)}{q_{f,0}} \tag{11}$$

Under complete liquefaction the maximum shear stress vanishes. This is assumed to take place when the damage indicator exceeds a critical value d_f. An appropriate assumption for the unknown function $f(D)$ then is

$$f(D) = \begin{cases} \left(1 - \left(\frac{D}{d_f}\right)^m\right) & , \quad D < d_f \\ 0 & , \quad D \geq d_f \end{cases} \tag{12}$$

Equation (12) does not describe the test results in every detail, and the value of m has to be estimated by experience. m seems to vary in the range 0.5-2.0.

STOCHASTIC DIFFERENTIAL EQUATIONS FOR HYSTERETIC SUBLAYER UNDER FILTERED WHITE-NOISE EXCITATION

Sublayer

The equation of motion relating the shear stress $\tau_{x'z'}(t)$ and the shear strain $\gamma_{x'z'}(t)$ just above the surface of the bedrock ($x' = 0$) can be written, see appendix A

$$\ddot{\gamma}_{x'z'} + \omega_0^2 \frac{\tau_{x'z'}}{\mu_{0,0}} = -a_0 \frac{\ddot{u}_g}{h} \tag{13}$$

ω_0 is the first cyclic eigenfrequency of the sublayer at zero damage, and a_0 is a non-dimensional constant dependent on the mode shape. Based on an approximate analysis expressions for these have been given in appendix A, assuming the mass density ρ to be constant in space and time.

The shear modulus at linear elastic deformations $\mu(x', D)$ at the damage state D is assumed to increase linearly from a minimum value $\mu_1(D)$ at the free surface to a maximum value $\mu_0(D)$ at the surface of the bedrock

$$\mu(x', D) = \mu_0(D) \left(1 - \left(1 - \frac{\mu_1(D)}{\mu_0(D)}\right) \frac{x'}{h}\right) \tag{14}$$

$\mu_0(D)$ and $\mu_1(D)$ decrease with time from initial values $\mu_{0,0}$ and $\mu_{1,0}$ as the damage develops. The fraction $\mu_1(D)/\mu_0(D) = \mu_{1,0}/\mu_{0,0}$ is assumed to be constant at all damage states, i.e. the stiffness deteriorates proportionally in top and bottom of the sublayer.

Using (4), (9), (11) equation (13) can be written

$$\ddot{x} + \frac{1}{2}\omega_0^2 f(D)\, z = -\omega_0^2\, v \tag{15}$$

where $f(D)$ is given by (12) and

$$v = \frac{a_0}{\omega_0^2 h} \frac{\mu_{0,0}}{q_{f,0}} \ddot{u}_g \tag{16}$$

The Bedrock Acceleration

Models for the bedrock acceleration $\ddot{u}_g(t)$, obtained by a linear filtering

of Gaussian shot noise, is well established in the literature, [1, 2]. In the following it is assumed that the frequency response function $H(\omega)$ of the shaping filter can be approximated with sufficient accuracy by a rational function, i.e.

$$H(\omega) = \frac{P(i\omega)}{Q(i\omega)} \tag{17}$$

where $P(z)$ and $Q(z)$ are polynomies of the degrees p and q, $0 \leq p \leq q$. The roots of $Q(z)$ have all negative real parts to ensure the stability and causality of the filter. (17) implies that the shaping filter is equivalent to a system of ordinary linear differential equations. In order to illustrate the method the following simple 2nd order filter ($p = 0, q = 2$) will be applied

$$\frac{d^2}{dt^2}\,\ddot{u}_g + 2\zeta\Omega_0 \frac{d}{dt}\,\ddot{u}_g + \Omega_0^2\,\ddot{u}_g = I(t)\,\frac{d}{dt}\,W(t) \tag{18}$$

ζ is the damping ratio, and Ω_0 is the undamped cyclic eigenfrequency of the filter.

$\{W(t), t \geq 0\}$ is a unit intensity Wiener process which is a Gaussian process with the following incremental properties

$$E[dW(t)] = 0 \quad , \quad E[dW(t_1)dW(t_2)] = \begin{cases} 0 & , \; t_1 \neq t_2 \\ dt & , \; t_1 = t_2 \end{cases} \tag{19}$$

$I(t)$ is a deterministic modulation function specifying the intensity of the white noise excitation process. It is assumed to be given by the following expression suggested by Saragoni and Hart, [9]

$$I(t) = I_0 \, \exp\!\left(-b\left(\frac{t}{T_0} - \ln\frac{t}{T_0} - 1\right)\right) \tag{20}$$

$$I_0 = \sqrt{4\zeta\Omega_0^3\,\sigma_{\ddot{u}_g}^0} \tag{21}$$

T_0 is the time of maximum intensity. The specification (21) ensures that the stationary standard deviation of $\ddot{u}_g$, in the case of stationary excitation with the intensity I_0, is equal to $\sigma_{\ddot{u}_g}^0$.

Introducing the non-dimensional acceleration v defined by (16), equation (18) can be written

$$\frac{d^2}{dt^2}\,v + 2\zeta\Omega_0 \frac{d}{dt}\,v + \Omega_0^2\,v = J(t)\,\frac{d}{dt}\,W(t) \tag{22}$$

$$J(t) = \frac{a_0}{\omega_0^2 h}\,\frac{\mu_{0,0}}{q_{f,0}}\sqrt{4\zeta\Omega_0^3}\,\sigma_{\ddot{u}_g}^0\,\exp\left(-b\left(\frac{t}{T_0} - \ln\frac{t}{T_0} - 1\right)\right) \tag{23}$$

Itô-Differential Equations

The state vector is made up of the state variables $x, \dot{x}, z$ of the sublayer, the damage indicator D, and the state variables $v, \dot{v}$ of the shaping filter. The integrated dynamical system as specified by (7,), (8), (10), (15), (22) can then be formulated by the following system of equivalent first order Itô-differential equations, [10].

$$d\mathbf{X}(t) = \mathbf{d}(\mathbf{X})dt + \mathbf{e}(t)dW(t) \quad , \quad t > t_0 \quad , \quad \mathbf{X}(t_0) = \mathbf{X}_0 \tag{24}$$

$$\mathbf{d}(\mathbf{X}) = \mathbf{A}(\mathbf{X})\mathbf{X} \tag{24a}$$

$$\mathbf{X}(t) = \begin{bmatrix} x \\ \dot{x} \\ z \\ D \\ v \\ \dot{v} \end{bmatrix} \quad \mathbf{e}(t) = \begin{bmatrix} 0 \\ 0 \\ 0 \\ 0 \\ 0 \\ J(t) \end{bmatrix} \tag{24b}$$

$$\mathbf{A}(\mathbf{X}) = \begin{bmatrix} 0 & 1 & 0 & 0 & 0 & 0 \\ 0 & 0 & -\frac{1}{2}\omega_0^2 f(D) & 0 & -\omega_0^2 & 0 \\ 0 & k(\dot{x}, z) & 0 & 0 & 0 & 0 \\ 0 & 4f(D)z & 0 & 0 & 0 & 0 \\ 0 & 0 & 0 & 0 & 0 & 1 \\ 0 & 0 & 0 & 0 & -\Omega_0^2 & -2\zeta\Omega_0 \end{bmatrix} \tag{24c}$$

The system is assumed to be undamaged before the earthquake excitation. The initial conditions are then $\mathbf{X}_0 = \mathbf{0}$.

RELIABILITY ANALYSIS

The probability of failure in the interval $[0,t]$ becomes

$$\begin{aligned} P_f([0,t]) &= 1 - P(\sup_{\tau\in[0,t]} D(\tau) \le d_f) \\ &= 1 - P(D(t) \le d_f) = 1 - F_{D(t)}(d_f) \end{aligned} \tag{25}$$

In the last statement of (25) it has been used that the sample curves of $D(t)$ are non-decreasing. Consequently, the probability of failure can be specified if the first order distribution function $F_{D(t)}(d)$ of $D(t)$ can

be determined. The lower order statistical moments of this quantity are estimated below.

EQUATIONS FOR JOINT CENTRAL MOMENTS FOR ORIGINAL AND EQUIVALENT SYSTEMS

Let $g(\mathbf{X}(t),t)$ be an arbitrary function of the state vector $\mathbf{X}(t)$ and t. Making use of the Itô-differential rule, and taking the expectation, the following differential equation for the expectation $E[g(\mathbf{X},t)]$ can be derived, [10]

$$\frac{d}{dt}E[g(\mathbf{X},t)] = E[\frac{\partial}{\partial t}g(\mathbf{X},t)]$$
$$+E[d_i(\mathbf{X})\frac{\partial}{\partial x_i}g(\mathbf{X},t)] + \frac{1}{2}e_ie_jE[\frac{\partial^2}{\partial x_i \partial x_j}g(\mathbf{X},t)] \tag{26}$$

In (26) and below the summation convention is used for dummy indices. d_i and e_i signify components of the drift-vector $\mathbf{d}(\mathbf{X})$ and of the diffusion-vector $\mathbf{e}$. Let

$$g(\mathbf{X},t) = \begin{cases} X_i & , \quad n=1 \\ X^c_{i_1}X^c_{i_2}\cdots X^c_{i_n} & , \quad n>1 \end{cases} \tag{27}$$

where $[X_1,X_2,X_3,X_4,X_5,X_6] = [x,\dot{x},z,D,v,\dot{v}]$ and

$$X^c_i = X_i - \mu_i \tag{28}$$

$$\mu_i = E[X_i] \tag{29}$$

Then

$$\dot{\mu}_i = E[d_i] \tag{30a}$$

$$\dot{\mu}_{ij} = E[d^c_iX^c_j] + E[d^c_jX^c_i] + e_ie_j \tag{30b}$$

$$\dot{\mu}_{ijk} = E[d^c_iX^c_jX^c_k] + E[d^c_jX^c_iX^c_k] + E[d^c_kX^c_iX^c_j] \tag{30c}$$

$$\dot{\mu}_{ijkl} = E[d^c_iX^c_jX^c_kX^c_l] + E[d^c_jX^c_iX^c_kX^c_l]$$
$$+E[d^c_kX^c_iX^c_jX^c_l] + E[d^c_lX^c_iX^c_jX^c_k]$$
$$+e_ie_j\mu_{kl} + e_ie_k\mu_{jl} + e_{il}\mu_{jk} + e_je_k\mu_{il} + e_je_l\mu_{ik} + e_ke_l\mu_{ij} \tag{30d}$$

where

$$d^c_i(\mathbf{X}) = d_i(\mathbf{X}) - E[d_i(\mathbf{X})] \tag{31}$$

$$\mu_{i_1 \cdots i_n} = E[X^c_{i_1} \cdots X^c_{i_n}] \tag{32}$$

Instead of the centralized drift vector of the original system, given by (31), an equivalent non-linear system is considered for which the centralized drift vector is given in terms of a quadratic expansion in the centralized state variables

$$d^c_{i,eq}(\mathbf{X}) = A_i + B_{im}X^c_m + C_{imn}X^c_m X^c_n + D_{imnp}X^c_m X^c_n X^c_p \tag{33}$$

The differential equations for the joint central moments of the equivalent system follow by inserting (33) into (30b)-(30d)

$$\dot{\mu}_{ij} = B_{im}\mu_{mj} + B_{jm}\mu_{mi} + C_{imn}\mu_{mnj} + C_{jmn}\mu_{mni}$$

$$D_{imnp}\mu_{mnpj} + D_{jmnp}\mu_{mnpi} + e_i e_j \tag{34a}$$

$$\dot{\mu}_{ijk} = A_i\mu_{jk} + A_j\mu_{ik} + A_k\mu_{ij} + B_{im}\mu_{mjk} + B_{jm}\mu_{mik} + B_{km}\mu_{mij}$$

$$+C_{imn}\mu_{mnjk} + C_{jmn}\mu_{mnik} + C_{kmn}\mu_{mnij}$$

$$+D_{imnp}\mu_{mnpjk} + D_{jmnp}\mu_{mnpik} + D_{kmnp}\mu_{mnpij} \tag{34b}$$

$$\dot{\mu}_{ijkl} = A_i\mu_{jkl} + A_j\mu_{ikl} + A_k\mu_{ijl} + A_l\mu_{ijk}$$

$$+B_{im}\mu_{mjkl} + B_{jm}\mu_{mikl} + B_{km}\mu_{mijl} + B_{lm}\mu_{mijk}$$

$$+D_{imnp}\mu_{mnpjkl} + D_{jmnp}\mu_{mnpikl} + D_{kmnp}\mu_{mnpijl} + D_{lmnp}\mu_{mnpijk}$$

$$+e_i e_j\mu_{kl} + e_i e_k\mu_{jl} + e_i e_l\mu_{jk} + e_j e_k\mu_{il} + e_j e_l\mu_{ik} + e_k e_l\mu_{ij} \tag{34c}$$

The system of differential equations (34) is not closed, because non-available joint central moments of the 5th and 6th order enter the right hand sides of (34b) and (34c). In the present case the differential equations will be closed using the cumulant neglect closure technique, assuming that the joint cumulants above the 4th order are negligible. This results in the following relationships for the joint central moments of the 5th and 6th order, [11]

$$\mu_{ijklm} = 15\{\mu_{ij}\mu_{klm}\}_s \tag{35}$$

$$\mu_{ijklmn} = 15\{\mu_{ij}\mu_{klmn}\}_s + 10\{\mu_{ijk}\mu_{lmn}\}_s - 30\{\mu_{ij}\mu_{kl}\mu_{mn}\}_s \tag{36}$$

The symbol $\{\cdot\}_s$ indicates a symmetry operation producing the arithmetic mean of all terms similar to those indicated, obtained by permuting all free indices.

For the non-analytical function $f(D)$ as given by (12) the following equivalent linearization, based on a Taylor-expansion from the mean value $\mu(D) = E[D]$, is used

$$f(D) = f(\mu_D) + f'(\mu_D)D^c, \quad D^c = D - \mu_D \tag{37}$$

(37) is used in the 4th equation of (24). For the 2th equation the approximation $f(D) = f(\mu_D)$ is used. From (24) the following tensor components in the equivalent system can then be obtained

$$\left.\begin{array}{l} B_{23} = -\frac{1}{2}\,\omega_0^2\, f(\mu_D) \\ A_4 = -4\, f(\mu_D)\, E[\dot{x}z] - 4\; f'(\mu_D)\, E[\dot{x}zD^c] \qquad C_{423} = 4\, f(\mu_D) \\ D_{4234} = 4\, f'(\mu_D) \end{array}\right\} \tag{38}$$

A_4 is obtained from the requirement $E[d^c_{3,eq}] = 0$. The remaining components of A_i, C_{imn} and D_{imnp} are all zero.

From eq. (7) the following symmetry property is obtained

$$k(\dot{x}, z) = k(-\dot{x}, -z) \tag{39}$$

(39) is known as the zero mean condition for white noise excited systems. In case of the initial conditions $\mathbf{X}_0 = \mathbf{0}$ the implication is that $E[\dot{x}] = E[z] = 0$, with the further implication that $\frac{d}{dt}E[z] = E[\dot{z}] = E[k(\dot{x}, z)\dot{x}] = 0$.

In agreement with the zero mean condition the following equivalent linear expansion is assumed for the constitutive equation

$$k(\dot{x}, z)\; \dot{x} = B_{32}\, \dot{x} + B_{33}\, z \tag{40}$$

The coefficients of the equivalent system are determined from the requirement that the expected value of the squared error $\epsilon = k(\dot{x}, z)\dot{x} - B_{32}\dot{x} - B_{33}z$ is at a minimum. The minimum conditions $\frac{\partial}{\partial B_{32}} E[\epsilon^2] = \frac{\partial}{\partial B_{33}} E[\epsilon^2] = 0$ result in the following linear equations for the determination of the expansion coefficients

$$\begin{bmatrix} E[\dot{x}^2] & E[\dot{x}z] \\ E[\dot{x}z] & E[z^2] \end{bmatrix} \begin{bmatrix} B_{22} \\ B_{32} \end{bmatrix} = \begin{bmatrix} E[k\dot{x}^2] \\ E[k\dot{x}z] \end{bmatrix} \tag{41}$$

The expectations on the right hand side of (41) are performed utilizing an approximate p.d.f. $f_{\dot{x}z}(\dot{x}, z)$. This is assumed in the form of a truncated 2-dimensional Gram-Charlier expansion, [12]

$$f_{\dot{x}z}(\dot{x}, z) = \frac{\varphi(\xi_2)}{\sigma_{\dot{x}}} \frac{\varphi(\xi_3)}{\sigma_z} \sum_{i+j=0}^{4} c_{ij} H_i(\xi_2) H_j(\xi_2) \tag{42}$$

where

$$\xi_2 = \frac{\dot{x}}{\sigma_{\dot{x}}} \quad , \quad \xi_3 = \frac{z}{\sigma_z} \tag{43}$$

$$H_i(\xi) = \sum_{\alpha=0}^{[\frac{i}{2}]} (-1)^{\alpha} a_{i,\alpha} \xi^{i-2\alpha} \ , \ a_{i,\alpha} = \frac{i!\, 2^{-\alpha}}{\alpha!(i-2\alpha)!} \tag{44}$$

$$\begin{aligned} c_{ij} &= \frac{1}{i!j!} E[H_i(\frac{\dot{x}}{\sigma_{\dot{x}}}) H_j(\frac{z}{\sigma_z})] \\ &= \frac{1}{i!j!} \sum_{\alpha_i=0}^{[\frac{i}{2}]} \sum_{\alpha_j=0}^{[\frac{j}{2}]} (-1)^{\alpha_i+\alpha_j} a_{i,\alpha_i} a_{j,\alpha_j} \frac{E[\dot{x}^{i-2\alpha_i}\ z^{j-2\alpha_j}]}{\sigma_{\dot{x}}^{i-2\alpha_i} \sigma_z^{j-2\alpha_j}} \end{aligned} \tag{45}$$

$\varphi(\cdot)$ is the frequency function of a standardized normal variable, and $H_i(\cdot)$ is the Hermite polynomium of the ith degree. For the expansion coefficients c_{ij} it follows that $vc_{00} = 1, c_{10} = c_{20} = c_{01} = c_{02} = 0$. Moreover $c_{ij} = 0, i + j$ is odd. The remaining coefficients follow from (45). The expectations on the right hand side of (41) can all be reduced to 1-dimensional quadratures.

The remaining components of B_{im} are equal to the linear components of matrix the **A**, given by (24c).

NUMERICAL EXAMPLE

The following data in agreement with test results have been used in the numerical study

$$\left.\begin{array}{llll} \omega_0 = 11.06\ \mathrm{s}^{-1} & , \ a_0 = 1.180 & , \ h = 30.5\ \mathrm{m} & \\ \rho = 1850\ \mathrm{kg/m}^3 & , \ \mu_{0,0} = 2.18 \cdot 10^8\ \mathrm{Pa} & , \ \mu_{1,0} = 2.18 \cdot 10^7\ \mathrm{Pa} & \\ \alpha = 1.0 & , \ \beta = 0.0 & , \ q_{f,0} = 2.42 \cdot 10^5\ \mathrm{Pa} & , \ n = 0.5 \\ b = 0.2 & , \ T_0 = 1\ \mathrm{s} & , \ \sigma_{\ddot{u}_g}^0 = 4.5\ \mathrm{m/s}^2 & \\ \Omega_0 = 15.56\ \mathrm{s}^{-1} & , \ \zeta = 0.458 & , \ m = 0.5 & , \ d_f = 119 \end{array}\right\} \tag{46}$$

To check the validity of the approximate analytical technique, response moments have been obtained from Monte-Carlo simulation based on averaging over 1000 independent sample curves, each obtained by numerical integration of eq. (24).

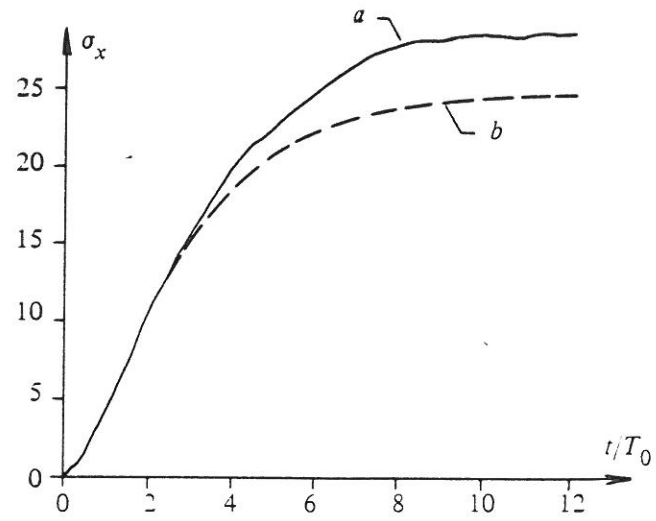

Figure 7. Standard deviation of x.

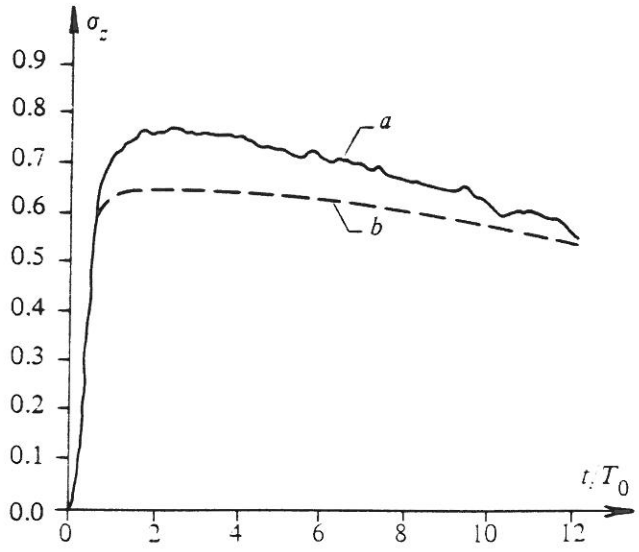

Figure 8. Standard deviation of z.

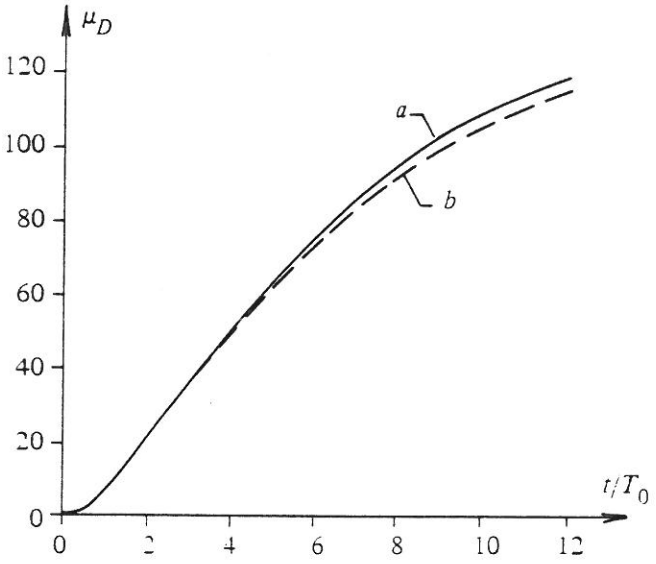

Figure 9. Mean value of D.

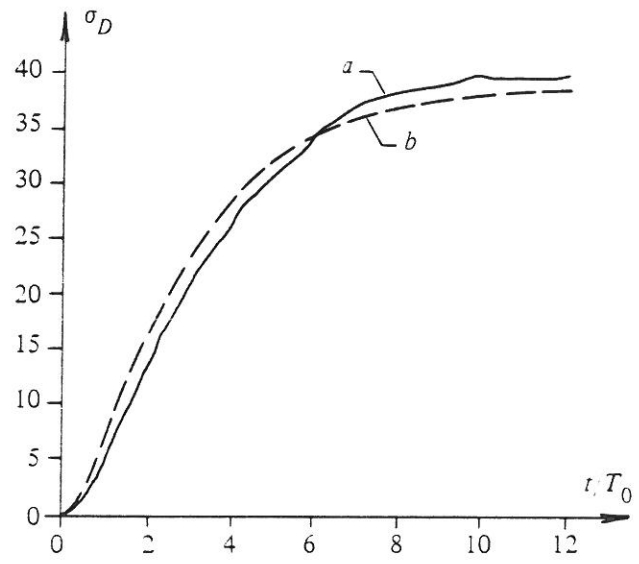

Figure 10. Standard deviation of D.

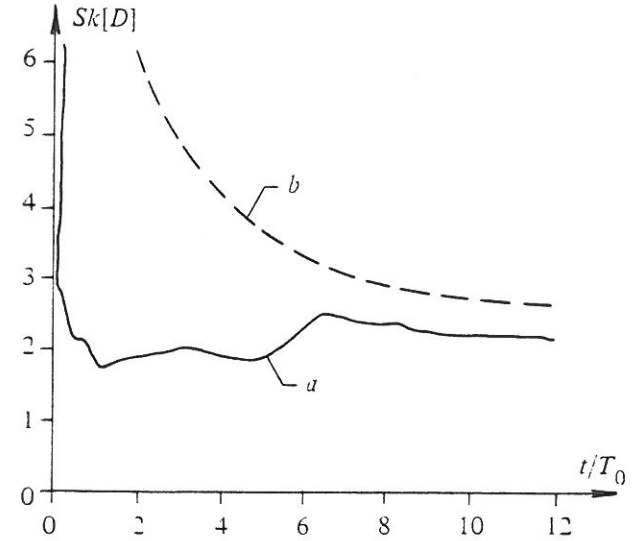

Figure 11. Skewness of D.

In the figures 7-11 time dependent response statistics for x, z and D have been shown. Curve a corresponds to simulation and curve b corresponds to equivalent polynomial expansion. The time has been normalized with respect to the period of linear eigenvibrations $T_0 = \frac{2\pi}{\omega_0}$.

In fig. 7 the time dependence on the standard deviation of x has been shown. Because μ_0/q_f is constant, x is proportional to the shear strain $\gamma_{x'z'}$, cf. (9). As seen the method provides a slight underestimation of the variance response of x.

In fig. 8 the standard deviation of z is shown. An acceptable agreement between simulated and analytically predicted results has been obtained. z is the shear stress in proportion to the deteriorating maximum stress, cf. (4). Due to this normalization, the decrease of the latter quantity is not displayed in the variance response of z. The slight decrease of z with time for $t/T_0 > 2$ should rather be asigned to the decreasing intensity of the excitation process, cf. (23).

Figures 9-11 show the time dependence on the mean value, standard deviation and skewness coefficient of the damage indicator D. The latter quantity is defined as $Sk[D] = E[(D - \mu_D)^3]/\sigma_D^3$. The severe earthquake considered with $\sigma_{\ddot{u}_g} = 4.5$ m/s^2 results in mean damage values exceeding 119 at the end of the interval considered, indicating a high risk for liquefaction. A good agreement between analytical and simulated results has been obtained for the mean value and for the standarddeviation, whereas the analytical values for the skewness are only acceptable for $t/T_0 > 8$.

However, the analysis shows, that the lower-order moments of D can be calculated by the indicated method, forming a basis for a succeeding reliability analysis.

CONCLUSIONS

A reliability analysis due to liquefaction of a hysteretic soil sublayer under earthquake excitation has been performed based on a Markov approach. A Bouc-Wen model is suggested as constitutive equation for the hysteretic shear stress, formulated in suitable normalized variables. Based on some promising cyclic triaxial tests the accumulated hysteretic energy dissipated in the soil is suggested as damage indicator. In the analytical approach an equivalent linearization technique is applied to the constitutive equation, and a cubic polynomial expansion based on a Taylor-expansion for the differential equation of the damage indicator. From the numerical example considered it is concluded, that the lower order statistical moments of the damage indicator can be estimated with sufficient accuracy by the indicated method.

Appendix A: Derivation of Eq. (13)

The equation of motion for a unit volume of the sublayer is

$$\frac{\partial \tau_{x'z'}}{\partial x'} = \rho \, \frac{\partial^2 u}{\partial t^2} \tag{A1}$$

The shear modulus is assumed to be given by the distribution in eq. (14). For the shear stress $\tau_{x'z'}(x',t)$ and the shear strain $\gamma_{x'z'}(x',t)$ the following single mode expansions are assumed

$$\tau_{x'z'}(x',t) = \tau_{x'z',0}(t) \left(1 - \left(1 - \frac{\mu_{1,0}}{\mu_{0,0}}\right) \xi\right) g'(\xi), \qquad \xi = \frac{x'}{h} \tag{A2}$$

$$\gamma_{x'z'}(x',t) = \gamma_{x'z',0}(t) \; g'(\xi) \tag{A3}$$

$g(\xi)$ is a non-dimensional shape function, and $g'(\xi)$ signifies the derivative with respect to ξ. $g(\xi)$ fulfils the boundary conditions $g(0) = g'(1) = 0$. Further $g(\xi)$ is normalized, so that $g'(0) = 1$. $\tau_{x'z',0}(t)$ and $\gamma_{x'z',0}(t)$ can then be interpreted as the shear stress and shear strain at the surface of the bedrock.

Integrating (A3), the following expression is obtained for the total displacement $u(x',t)$

$$u(x',t) = u_g(t) \; + \; \gamma_{x'z',0}(t) \; h \; g(\xi) \tag{A4}$$

(A1) is multiplied by a virtual displacement $\delta u(x',t)$. Partial integration and application of the boundary conditions at $x' = 0$ and $x' = h$ provides

$$-\int_0^h \tau_{x'z'} \; \delta\gamma_{x'z'} \; dx' \; = \; \int_0^h \rho \; \ddot{u} \; \delta u \; dx' \qquad \Rightarrow$$

$$\ddot{\gamma}_{x'z',0} \; + \; \omega_0^2 \; \frac{\tau_{x'z',0}}{\mu_{0,0}} \; = \; -a_0 \; \frac{\ddot{u}_g}{h} \tag{A5}$$

$$\omega_0^2 \; = \; \frac{\int_0^1 \left(1 - \left(1 - \frac{\mu_{1,0}}{\mu_{0,0}}\right)\xi\right) \left(g'(\xi)\right)^2 \, d\xi}{\int_0^1 g^2(\xi) \; d\xi} \; \frac{\mu_{0,0}}{\rho h^2} \; = \; \left(1.620 \; \frac{\mu_{0,0}}{\rho h^2}\right) \tag{A6}$$

$$a_0 \; = \; \frac{\int_0^1 g(\xi) \; d\xi}{\int_0^1 g^2(\xi) \; d\xi} \; = \; (1.180) \tag{A7}$$

In the main text the index 0 on $\tau_{x'z',0}$ and $\gamma_{x'z',0}$ has been omitted. As shape function the first eigenvibration mode is used, fulfilling the eigenvalue problem

$$\left.\begin{array}{l} \frac{d}{d\xi}\left((1-\left(1-\frac{\mu_{1,0}}{\mu_{0,0}}\right)\xi)\,\frac{d}{d\xi}\,g(\xi)\right)+\frac{\rho h^2}{\mu_{0,0}}\,\omega_0^2\,g(\xi) \\ g(0)=g'(1)=0 \quad , \quad g'(0)=1 \end{array}\right\} \tag{A8}$$

The solution to ω_0^2 and a_0 for $\frac{\mu_{1,0}}{\mu_{0,0}} = 0.1$ has been given in the parentheses of (A6) and (A7).

REFERENCES

[1] Newmark, N. M. & E. Rosenblueth: *Fundamentals of Earthquake Engineering*, Prentice-Hall, Inc., 1971.

[2] Boore, D. M.: *Stochastic Simulation of High-Frequency Ground Motions Based on Seismological Models of the Radiated Spectra*, Bull. Seismological Soc. Am., Vol. 73, No. 6, pp. 1865-1894, 1983.

[3] Spanos, P. - T. D.: *Formulation of Stochastic Linearization for Symmetric or Asymmetric MDOF Nonlinear Systems*, J. Appl. Mech., ASME, Vol. 47, No. 1, pp. 209-211, 1980.

[4] Baber, T. T.: *Nonzero Mean Random Vibration of Hysteretic Systems*, J. Eng. Mech., ASCE, Vol. 110, No. 7, pp. 1036-1049, 1984.

[5] Nielsen, S. R. K., K. Mørk & P. Thoft-Christensen: *Response of Hysteretic Multi-Storey Frames under Earthquake Excitation.* Structural Reliability Theory, Paper No. 41, ISSN 0902-7513 R8805, University of Aalborg, Denmark, 1988 (to appear in Earthquake Eng. Struct. Dyn., 1989).

[6] Mørk, K.: *Stochastic Response and Reliability Analysis of Hysteretic Structures.* Structural Reliability Theory, Paper No. 56, ISSN 0902-7513 R8910, University of Aalborg, Denmark, 1989 (Ph.D. thesis).

[7] Ibsen, L.B. & Jacobsen, H.M.: *Cyclic Triaxial Tests on Sand. Hysteretic Curves and Dissipated Mechanical Energy.* University of Aalborg, Denmark, 1989.

[8] Wen, Y.- K.: *Method for Random Vibration of Hysteretic Systems*, J. Eng. Mech., ASCE, Vol. 102, pp. 249-263, 1976.

[9] Saragoni, G. R. & G. C. Hart: *Simulation of Artificial Earthquakes*, Earthquake Eng. Struc. Dyn., Vol. 2, pp. 249-267, 1974.

[10] Arnold, L.: *Stochastic Differential Equations: Theory and Applications*, John Wiley & Sons, 1974.

[11] Stratonovich, R. L.: *Topics in the Theory of Random Noise, Vol. 1*, Gordon and Breach, 1963.

[12] Cramér, H.: *Mathematical Methods of Statistics*, Princeton University Press, Princeton, 1946.

[13] Peacock, W.H. & Seed, H.B.: *Sand Liquefaction Under Cyclic Loadings Simple Shear Conditions*. J. Soil Mech. Found. Div., ASCE, Vol. 94. pp. 689-708, 1968.

[14] Casagrande, A.: *On Liquefaction Phenomena*. Geotechnique, Vol XXI, No. 3, pp. 197-202, Sept., 1971.

[15] Castro, G.: *Liquefaction and Cyclic Mobility of Saturated Sands*. J. Geo. Eng. Div., ASCE, Vol. 101, pp. 551-569, 1975.

[16] Jacobsen, H.M. & Ibsen, L.B.: *Development of Porepressure in Cohesionless Soils with Initial Shear Stresses During Cyclic Loading*. to appear in Proceedings, YGEC III, Minsk, 1989.